SMALL IMPACTS TRIGGER DUST LANDSLIDES ON MARS. K.J. Burleigh[1], H.J. Melosh[1], L.L. Tornabene[1], and A.S. McEwen[1], [1]Lunar and Planetary Lab, University of Arizona, Tucson AZ 85721 (kaylanb@email.arizon.edu).

Introduction: The HiRISE imaging system recently confirmed the suggestion from MOC [1] that new small (~1 km diameter) dark spots on Mars are the sites of recent (< 10 years old) small impact craters. At present, >70 such impacts have been imaged by the HiRISE system at scales ranging from 0.25 to 0.32 m/pixel. All of these new impact sites have been discovered over dust-mantled regions where small impacts produce dark spots that are easily detected from orbit. Our work focuses on a small impact in PSP_002764_1800. The impact produced a cluster of five relatively large craters and several smaller craters, of which the largest is ~21.7 m in diameter, located at 0^o 1' 56.81" S, 226^o 55' 30.61" E. This crater cluster formed in plains of the Amazonian Upper Medusae Fossae formation [2,3], initiating approximately 10^5 small landslides on steep slopes of apparent yardangs that traverse the HiRISE image [4]. This impact site was re-imaged 230 days later via PSP_005665_1800 and appears unchanged except for different illumination angles. This region has a high albedo and low thermal inertia inidicative of a dust cover.

We classified and mapped the location and orientation of 64,336 small landslides in the vicinity of the impact and computed the spatial density of the landslides as a function of distance from the largest crater. Our goal is to determine whether the impact caused the landslides and to discriminate between two possible trigger mechanisms: Seismic shaking or airblast-induced slope failure.

Method: We superimposed a 500 m x 500 m grid over the image to establish consistent areas for landslide counting. Five classes of landslides, CL1-CL4, and CLFaint, were defined based on their relative albedo and morphology (Figure 1). CL1 are dark, with sharply defined edges, longitudinal grooves, well-defined headscarps and downslope deposits. CL2 are similar to CL1, but lack obvious grooves and have higher albedos. CL3 are typically less than half as long as CL1 and CL2s, have higher albedo and lack well-defined headscarps. CL4 possess degraded margins, the highest albedo and a mottled appearence. CLFaint are blurred, narrow, and faint with higher albedos.

Using Environment for Visualizing Images (ENVI v4.5), we defined a grid system North (N), South (S), and West (W) of the impact that encompass the majority of the landslides. The N region was 3x6 cells, the S: 3x5, and the W: 3x7. Line segments were drawn on the image to locate and classify each type of landslide.

Results: The impact fell nearly on the boundary between two distinct terrains. To the N are ridges, interpreted as mega-yardangs, spaced ca. 375 m apart, while to the S the terrain is dissected into meso-yardangs spaced at ca. 25 m. The difference in spacing of the ridges is reflected in a difference in the average lengths of the landslides: Slopes are longer in the N quadrant and so the landslides are both longer and less numerous in this direction: an average spatial density of types CL1-CL3 of 2,836 km^{-2} in the N, compared to 5,141 km^{-2} in the S and 5,987 km^{-2} to the W. The S lies entirely in the finer-textured terrain and 14 out of 21 grid cells in the W lie in this terrain.

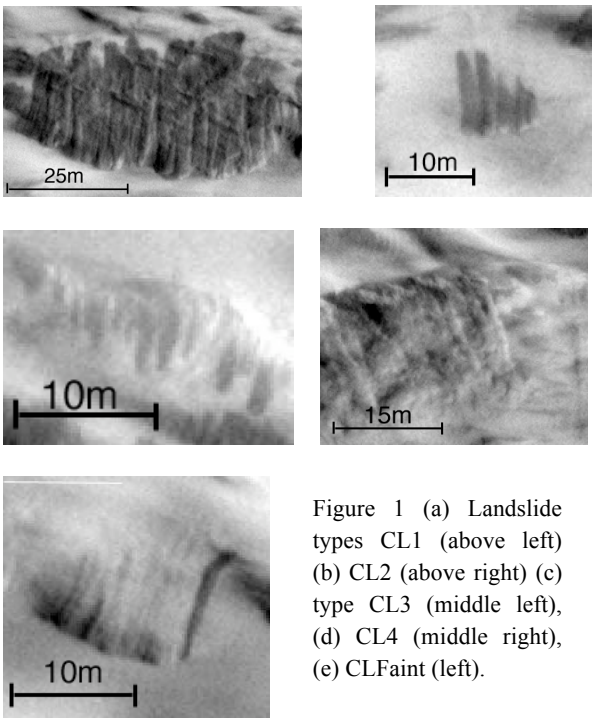

Figure 1 (a) Landslide types CL1 (above left) (b) CL2 (above right) (c) type CL3 (middle left), (d) CL4 (middle right), (e) CLFaint (left).

The spatial density of CL1-CL3 landslides is highest closest to the impact crater cluster, reaching a maximum of 14,464 km^{-2}, dropping to near zero farther than about 2 km from the impact site (Figure 2). These landslide types are correlated with proximity to the impacts and therefore, we infer that they were triggered by the impact event. The density of type CL4 reaches a maximum of 160 km^{-2} but does not appear to correlate with distance from the impact site: We interpret these as pre-impact features.

Type CLFaint landslides anticorrelate with types CL1-CL3 (Figure 3): They are apparently absent near the impact and their density increases sharply to about

800 km^{-2} beyond about 1.5 km from the impact site to the S and beyond 2.2 km in the N. No increase is apparent in the W, where the boundary of the image strip was reached. We believe these landslides predated the impact and were replaced or reactivated by CL1-CL3.

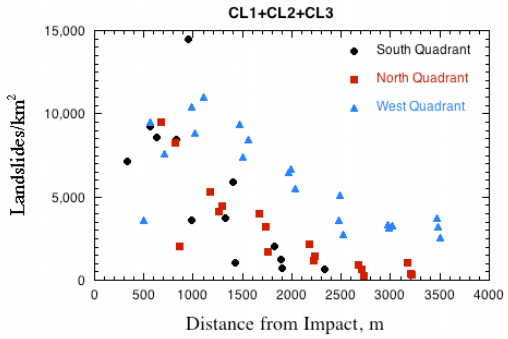

Figure 2. Landslide number density vs. distance.

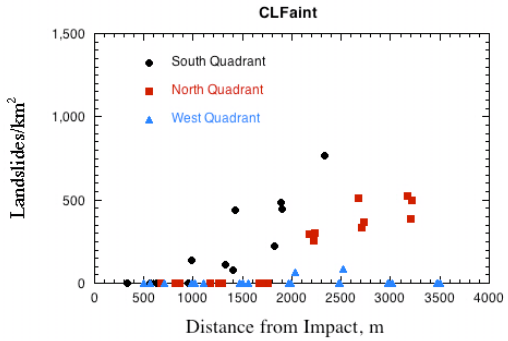

Figure 3. Anticorrelation of type CLFaint with distance.

A crucial observation relevant to the trigger mechanism is provided by a narrow curved, scimitar-like albedo feature stretching 1.85 km S of the impact site (a fainter symmetric feature can also be seen to the N). This feature is too narrow to be attributed to seismic shaking, but is likely due to interference between the direct and surface-reflected air shocks of the incoming bolide. We found that the high-albedo part of this feature contains very few landslides, whereas a parallel dark margin to the east has an exceptionally high density, especially of CL2 landslides (the low albedo of this feature appears to be entirely due to the large density of the landslides: A similar trend in CL2 is seen in the faint symmetric feature to the N). Because seismic shaking is unlikely to vary substantially between the two adjacent portions of this narrow feature, we infer that the landslides were mainly triggered by the airblast, not seismic shaking.

We fitted power law and exponential functions to the number density of types CL1-CL3 vs. distance. The fits of the power laws range from -1.4 to -1.9 using all the data (or -1.9 to -2.1 excluding outlying points) for the S and N quadrants, respectively, but the goodness of fit is poor (R=0.46 and 0.86, respectively). An exponential decay with distance offers marginally better fits. The decline to the W is substantially less rapid for either type of fit: -0.6 (R=0.56) for a power law—or -1.1 (R=0.72) with outliers removed—and less than ½ the rate for an exponential decay. The slower decay to the W may be due to coincidence with the approach path of the impactor, consistent with an airblast-induced landslide origin.

Conclusions: The strong correlation between the density of fresh landslide types CL1-CL3 and the site of the recent small impact implies that the landslides were triggerd directly by the impact itself. The low albedo of these landslides is due to the exposure of darker underlying material. The appearance of the grooves and the deposits at the toe of type CL1 landslides suggest that they excavated at least 10's of cm of underlying material.

The anti-correlation between CL1-CL3 and CLFaint suggest that CLFaint are pre-existing landslides whose high albedo is due to the gradual deposition of dust on Mars' surface. CLFaint are apparently reactivated or overprinted by the fresh CL1-CL3 types.

The strong correlation between landslide density and the albedo variations of the "scimitar" feature indicate that, if this feature originated from airblast shock interference, then the principal trigger for landslide formation was an airblast, not seismic shaking.

Finally, the enormous area affected by the impact (100 times larger than the crater diameter) suggests that surface modification by small impacts is far more significant than previously thought. Our crater cluster was probably caused by an impactor ca. 1 m in diamter. Assuming a Martian cratering rate similar to Earth's [5], any point on the Martin surface is subjected to a similar landslide-triggering event every ~2 million years. Every point on the plains of the Medusae Fossae formation was thus affected by a similar event approximately 50 times since its formation [ref]; with older regions on Mars suffering a proportionately larger number of events. However, regions without a recent dust cover may be largely unaffected.

References: [1] Malin, M. C. et al. (2006), *Science* **314**, 1573. [2] Scott, D. H. and Tanaka, K. L. (1986), USGS Map I-1802-A. [3] Scott, D. H. et al. (1981), USGS Map I-1268. [2] Chuang, F. C., et al. (2007), GRL **34**, L20204. [5] NEO Science Definition Team (2003), Study to Determine the Feasibility of Extending the Search for Near-Earth Objects to Smaller Limiting Diameters. NASA Technical Report.